Extensive meiotic asynapsis in mice antagonises meiotic silencing of unsynapsed chromatin and consequently disrupts meiotic sex chromosome inactivation

Shantha K. Mahadevaiah,[1] Déborah Bourc'his,[2] Dirk G. de Rooij,[3,4] Timothy H. Bestor,[5] James M.A. Turner,[1] and Paul S. Burgoyne[1]

[1]Division of Stem Cell Biology and Developmental Genetics, Medical Research Council National Institute for Medical Research, London NW7 1AA, England, UK
[2]Institut National de la Santé et de la Recherche Medicale U741, Institut Jacques Monod, 75251 Paris, Cedex 05, France
[3]Center for Reproductive Medicine, Academic Medical Center, University of Amsterdam, Amsterdam 1105 AZ, Netherlands
[4]Department of Endocrinology and Metabolism, Faculty of Science, Utrecht University, Utrecht 3584 CH, Netherlands
[5]Department of Genetics and Development, College of Physicians and Surgeons of Columbia University, New York, NY 10032

Chromosome synapsis during zygotene is a prerequisite for the timely homologous recombinational repair of meiotic DNA double-strand breaks (DSBs). Unrepaired DSBs are thought to trigger apoptosis during midpachytene of male meiosis if synapsis fails. An early pachytene response to asynapsis is meiotic silencing of unsynapsed chromatin (MSUC), which, in normal males, silences the X and Y chromosomes (meiotic sex chromosome inactivation [MSCI]). In this study, we show that MSUC occurs in *Spo11*-null mouse spermatocytes with extensive asynapsis but lacking meiotic DSBs. In contrast, three mutants (*Dnmt3l*, *Msh5*, and *Dmc1*) with high levels of asynapsis and numerous persistent unrepaired DSBs have a severely impaired MSUC response. We suggest that MSUC-related proteins, including the MSUC initiator BRCA1, are sequestered at unrepaired DSBs. All four mutants fail to silence the X and Y chromosomes (MSCI failure), which is sufficient to explain the midpachytene apoptosis. Apoptosis does not occur in mice with a single additional asynapsed chromosome with unrepaired meiotic DSBs and no disturbance of MSCI.

Introduction

The discovery of the phenomenon of meiotic silencing of unsynapsed chromatin (MSUC; Baarends et al., 2005; Turner et al., 2005) followed from studies of meiotic sex chromosome inactivation (MSCI), the transcriptional silencing of unsynapsed regions of the XY bivalent during pachytene of normal male meiosis, the morphological correlate of which is the so-called sex or XY body (Handel, 2004; Turner and Burgoyne, 2007). It is now clear that MSCI is an MSUC response to unsynapsed chromosomal regions (Turner et al., 2006). Three key steps have been identified that trigger the chromatin changes resulting in MSCI/MSUC (Turner et al., 2004, 2005). First, there is an accumulation of the DNA damage response protein BRCA1 on the unsynapsed chromosome axis (Scully et al., 1997; Turner et al., 2004, 2005). This is followed by a BRCA1-dependent axial accumulation of the PI3K kinase ataxia telangiectasia and Rad3 related (ATR), which then spreads throughout the chromatin associated with the unsynapsed axis (Turner et al., 2004, 2005). ATR then phosphorylates serine 139 of the variant nucleosomal histone H2AX (Turner et al., 2004; Bellani et al., 2005), and it is this phosphorylation event that triggers the chromatin changes that lead to transcriptional silencing (Fernandez-Capetillo et al., 2003). BRCA1 and ATR are also key players in the checkpoint management of double-strand breaks (DSBs) during G2 of mitosis (Lisby and Rothstein, 2005) and are thought to play a similar checkpoint role in meiosis because they localize

Correspondence to Paul S. Burgoyne: pburgoy@nimr.mrc.ac.uk

Abbreviations used in this paper: ATR, ataxia telangiectasia and Rad3 related; BAC, bacterial artificial chromosome; DSB, double-strand break; MSCI, meiotic sex chromosome inactivation; MSUC, meiotic silencing of unsynapsed chromatin; SCD, SQ/TQ cluster domain.

The online version of this article contains supplemental material.

The Rockefeller University Press $30.00
J. Cell Biol. Vol. 182 No. 2 263–276
www.jcb.org/cgi/doi/10.1083/jcb.200710195

to meiotic DSBs during leptotene and zygotene before being shed soon after the completion of homologue synapsis and DSB repair (Keegan et al., 1996; Scully et al., 1997; Moens et al., 1999; Turner et al., 2004; for review see Burgoyne et al., 2007). It is for this reason that the accumulation of BRCA1 and ATR during pachytene on chromosomal axes that fail to synapse and, thus, the resulting MSUC response have also been assumed to be DSB dependent (Perera et al., 2004). However, although the presence of DSB markers (e.g., RAD51) on the unsynapsed X chromosome axis indicates that there are multiple meiotic DSBs present throughout most of pachytene (Moens et al., 1997; Plug et al., 1998), such markers are rarely seen on the unsynapsed Y chromosome axis; nevertheless, the Y is subject to MSCI/MSUC (Turner et al., 2004, 2005, 2006).

Importantly, two studies of *Spo11*-null male meiosis revealed that the sex body–like structure apparent in *Spo11*-null pachytene spermatocytes rarely encompassed the X or Y (Barchi et al., 2005; Bellani et al., 2005). However, neither study established whether this was associated with MSCI failure, whether the "pseudo–sex body" domain was transcriptionally silenced, or whether it was targeted to asynapsed chromatin. Because we now know that MSCI is a manifestation of the MSUC response (Turner et al., 2006), resolution of these issues is important to allow any conclusion as to whether MSUC can be provoked by asynapsis in the absence of meiotic (i.e., *Spo11* dependent) DSBs.

Results

An MSUC response occurs in *Spo11*-null males, but there is extensive MSCI failure

To test whether the MSUC response can occur independently of meiotic DSBs, we looked for an MSUC response in *Spo11*-null male meiosis in which the lack of the SPO11 DNA transesterase prevents meiotic DSB formation (Fig. S1, a–f; available at http://www.jcb.org/cgi/content/full/jcb.200710195/DC1; Romanienko and Camerini-Otero, 2000; Baudat et al., 2000; Mahadevaiah et al., 2001). In these males, the lack of meiotic DSBs severely disrupts homologous synapsis, and although there is some nonhomologous synapsis at or after the zygotene/pachytene transition (a meiotic DSB-independent default synapsis; Zickler and Kleckner, 1999), many chromosome axes remain unsynapsed until the pachytene spermatocytes are eliminated by apoptosis.

We first immunostained spread *Spo11*$^{-/-}$ meiotic cells for BRCA1 and for the synaptonemal complex protein SYCP3 (which is loaded onto the chromosome axes before synapsis); the pattern of SYCP3 staining allows an assessment of meiotic stage. Unexpectedly, BRCA1, which is known to localize to meiotic DSBs (Scully et al., 1997), was clearly detectable as foci on the chromosome axes in *Spo11*$^{-/-}$ leptotene and zygotene spermatocytes despite the lack of meiotic DSBs (Fig. 1, e and f). The BRCA1 staining was initially comparable with that in controls (Fig. 1, a and b). Foci were not visible in spermatocytes from *Brca1*$^{\Delta 11/\Delta 11}$,*Trp53*$^{+/-}$ mutant males that produce a shortened protein lacking the exon 11–encoded region, against which the BRCA1 antibody is raised (Fig. 1, i and j; Xu et al., 2003; Turner et al., 2004). As previously reported (Scully et al., 1997; Turner et al., 2004), in wild-type males, the DSB-associated BRCA1 was lost after synapsis and during pachytene accumulated on the asynapsed axes of the X and Y chromosomes (Fig. 1, b and c). Similarly, in *Spo11*$^{-/-}$ spermatocytes, BRCA1 disappeared from the axes in conjunction with nonhomologous synapsis, which initiates at the zygotene–pachytene transition (Fig. 1 g, inset). It then accumulated during early pachytene on the chromosome axes of a restricted chromatin domain (Fig. 1 g); this is the domain within which ATR accumulates and phosphorylation of H2AX occurs (Fig. 1 h; Mahadevaiah et al., 2001; Bellani et al., 2005). This domain has been termed the pseudo–sex body because it resembles the inactivated XY chromatin domain in wild-type pachytene spermatocytes (Fig. 1 d) but is not restricted to X and Y chromatin (Barchi et al., 2005; Bellani et al., 2005).

Although the formation of a pseudo–sex body in *Spo11*$^{-/-}$ pachytene spermatocytes is consistent with an MSUC response, it seemed clear that the extent of this domain was not consonant with the extensive asynapsis. To confirm this, we performed immunostaining for ATR and SYCP3 together with the synaptonemal complex protein SYCP1 that locates to regions of synapsis (whether homologous or nonhomologous). In all 50 pachytene cells analyzed, the ATR domain was found to be excluded from SYCP1-positive axes and associated chromatin; nevertheless, there were many unsynapsed chromosomal regions that were devoid of ATR (Fig. 1, k and l). We conclude that the pseudo–sex body in *Spo11*$^{-/-}$ pachytene spermatocytes is targeted to unsynapsed chromatin but fails to encompass all such chromatin.

We then asked whether the γH2AX-positive pseudo–sex body domain was transcriptionally repressed by use of a Cot1 probe to detect nascent transcripts (Turner et al., 2005) and then immunostained for γH2AX to locate the pseudo–sex body domain. This showed that the γH2AX domain was indeed transcriptionally repressed in cells that had a clear pseudo–sex body (Fig. 2, a and b). We next combined γH2AX immunostaining with RNA FISH and DNA FISH for *Atr*, which is autosomal and in wild-type males is robustly expressed throughout pachytene (Fig. S2, a–e; available at http://www.jcb.org/cgi/content/full/jcb.200710195/DC1). It was predicted that any pachytene cells with an *Atr* locus that failed to transcribe would have the *Atr* locus within the transcriptionally repressed γH2AX domain. 7/42 (17%) pachytene cells had one transcribed and one nontranscribed *Atr* locus, and, in each case, the nontranscribing locus was within the γH2AX-positive region (Fig. 2, c and d). We next performed RNA FISH analysis for the Y-located gene *Zfy2* that in normal males is weakly expressed in leptotene and zygotene spermatocytes when chromatin condensation is associated with global transcriptional repression and is then shut down by MSCI/MSUC throughout pachytene (Fig. S2, k–o). This revealed that 70/74 (95%) *Spo11*$^{-/-}$ pachytene cells were inappropriately expressing *Zfy2* (Fig. 2, e and f); in 69 of these cells, the *Zfy2* locus was located away from the γH2AX-positive domain, and one weakly expressed locus was at the edge of the domain. In the four nonexpressing cells, the *Zfy2* locus was located within the γH2AX-positive domain (Fig. 2, g and h). Finally, we performed RNA FISH analysis using an X-chromosomal bacterial artificial

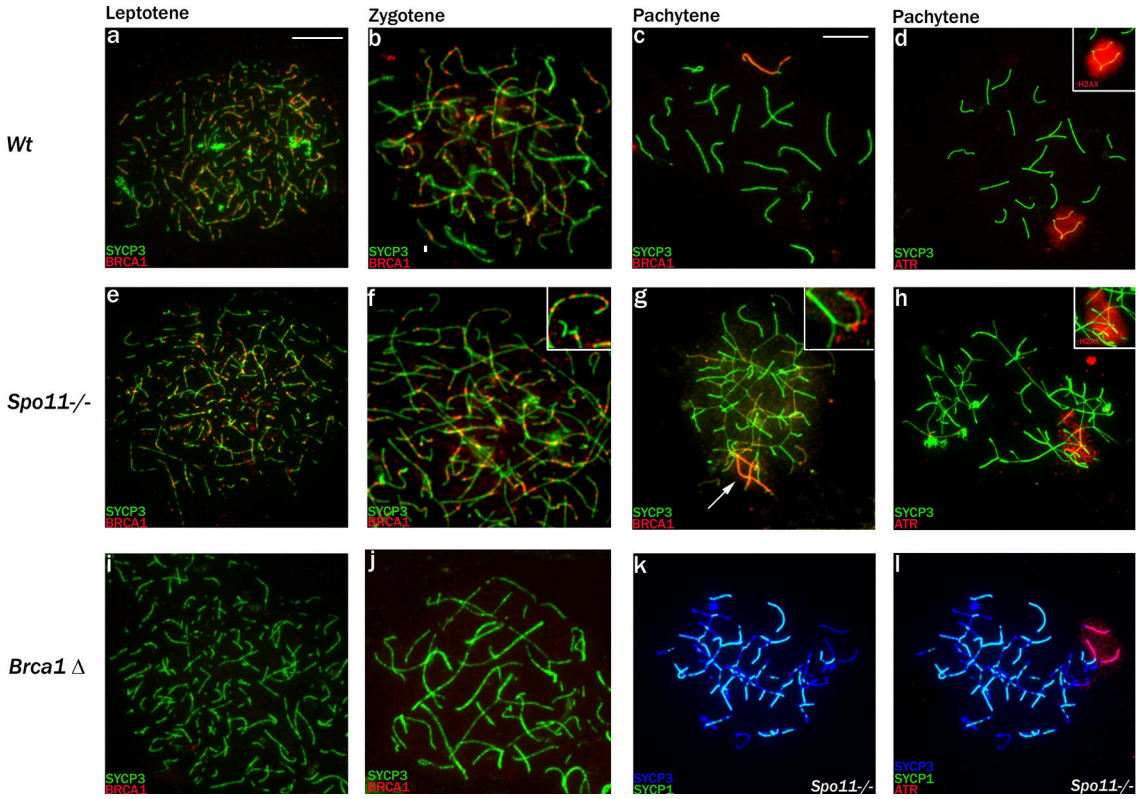

Figure 1. **The MSUC initiator proteins BRCA1 and ATR are recruited to the pseudo–sex body domain of *Spo11*-null pachytene spermatocytes.** (a–c) SYCP3 and BRCA1 staining of control spermatocytes showing the appearance of BRCA1 foci on the forming axial elements in leptotene, their loss after synapsis during zygotene, and BRCA1 accumulation on the asynapsed X and Y axes in pachytene. (d) The kinase ATR appears throughout the chromatin of the asynapsed X and Y axes in pachytene of control males, and there is an associated phosphorylation of H2AX (γH2AX), which defines the sex body domain (inset). (e–g) In *Spo11*-null spermatocytes, which lack meiotic DSBs, BRCA1 foci still appear on the axial elements in leptotene, are retained throughout the asynaptic zygotene stage (magnified in insets), and are lost in conjunction with the nonhomologous synapsis apparent in pachytene (highlighted in insets, which show synapsed and asynapsed axes with BRCA1 staining offset). There is concurrent BRCA1 accumulation on a subset of asynapsed axes (arrow) that mark the location of the pseudo–sex body. (h) Staining with ATR or γH2AX (inset) marks the entire chromatin domain of the pseudo–sex body. (i and j) In *Brca1*$^{\Delta 11/\Delta 11}$,*Trp53*$^{+/-}$ leptotene and zygotene spermatocytes, no foci are detected, confirming the specificity of the BRCA1 antibody. (k and l) A *Spo11*-null pachytene spermatocyte stained with SYCP3 and SYCP1. The synapsed regions appear light blue because of colocalization; the pseudo–sex body domain marked with ATR is restricted to the chromatin of asynapsed axes but only encompasses a small proportion of such chromatin. Bars, 10 μm.

chromosome (BAC) probe encompassing *Ddx3x* and 28 kb of *Usp9x*. We have found that this BAC gives no detectable RNA FISH signal in normal spermatocytes (Figs. S2, p–t; and S4, a and b); however, in *Brca1*$^{\Delta 11/\Delta 11}$ males (which have extensive MSCI failure; Turner et al., 2004), a *Ddx3x/Usp9x* signal becomes progressively more evident during pachytene (Figs. S3, g–i; and S4, c and d). This provides a robust pachytene-specific marker of MSCI failure but will underestimate the proportion of pachytene cells with MSCI failure because transcription does not commence immediately upon entry of cells into pachytene. In *Spo11*$^{-/-}$ males, 36/43 (84%) pachytene cells were found to be inappropriately expressing *Ddx3x/Usp9x* because the locus was not within the γH2AX-positive domain (Fig. 2, i–l). In four of the seven nonexpressing cells, the *Ddx3x/Usp9x* locus lay within the γH2AX domain (Fig. 2, m and n).

These results show that an MSUC response does occur within the pseudo–sex body domain of *Spo11*$^{-/-}$ pachytene spermatocytes, and the MSUC response can occur in the absence of *Spo11*-dependent (meiotic) DSBs. Because the MSUC response is not specifically targeted to the unsynapsed X and Y axes, most (>84%) *Spo11*$^{-/-}$ pachytene spermatocytes have MSCI failure.

The MSUC response is increasingly impaired as asynapsis increases in spermatocytes that lack DNMT3L

Conceivably, the spatially limited MSUC response in *Spo11*$^{-/-}$ pachytene spermatocytes could be caused by the lack of meiotic DSBs, with some localized meiotic DSB-independent DNA damage serving to nucleate BRCA1 accumulation and thus trigger the localized MSUC response. If so, pachytene cells with extensive asynapsis that is associated with widespread, unrepaired meiotic DSBs should mount a more complete MSUC response. *Dnmt3l*-null males are very unusual in that progression to meiotic prophase is only seen before puberty, after which there is progressively earlier spermatogenic failure as a result of the progressive depletion of early proliferating spermatogonial stages (Bourc'his et al., 2001; Hata et al., 2002; Webster et al., 2005; La Salle et al., 2007). Homologous chromosome synapsis is substantially impaired (Bourc'his and Bestor, 2004; Webster et al., 2005; Hata et al., 2006), yet there are numerous meiotic DSBs (Fig. S1, g–i).

Combined SYCP3, γH2AX, and ATR immunostaining indicated that in pachytene cells with limited asynapsis, there was a

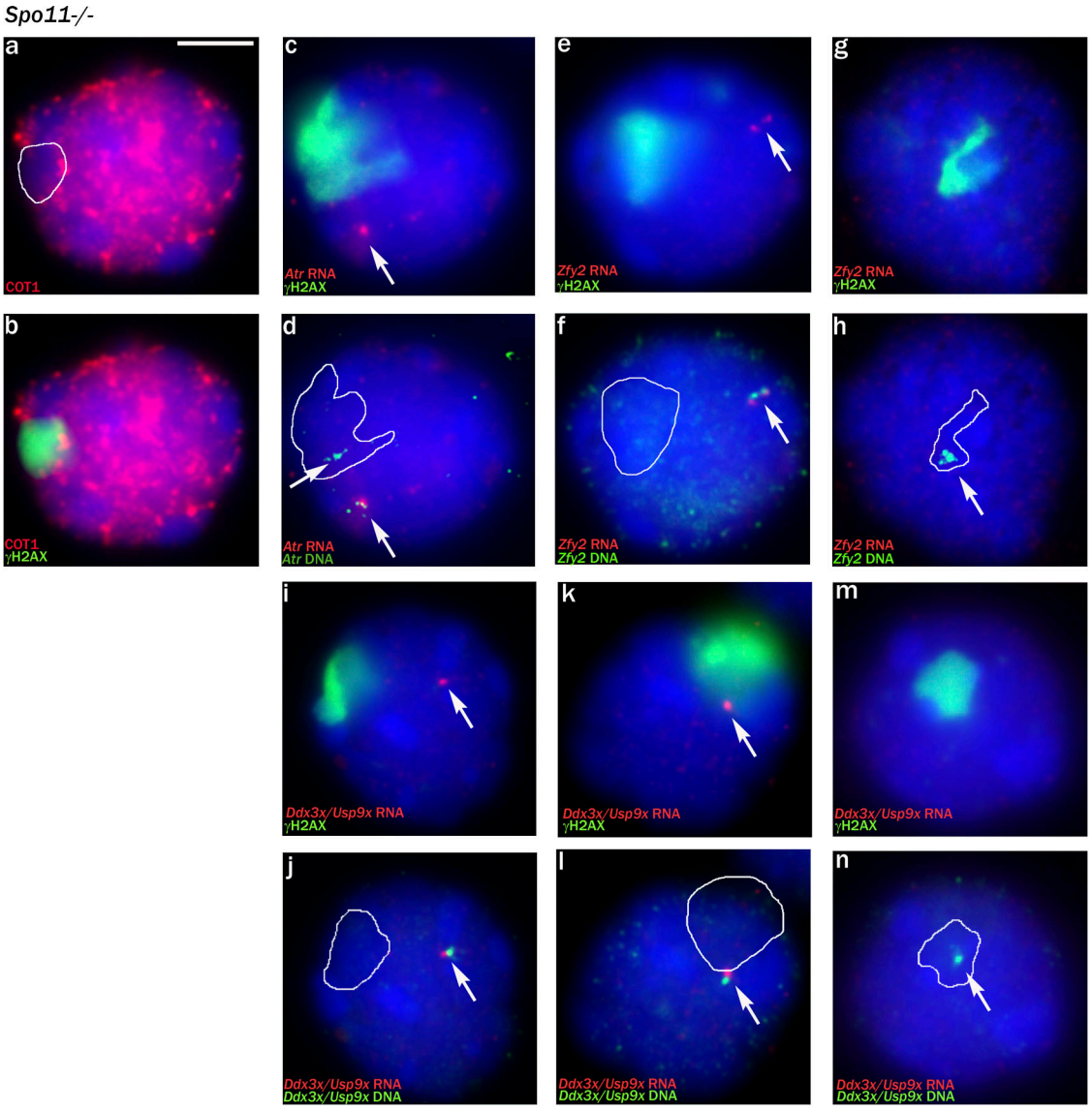

Figure 2. **The pseudo–sex body domain of *Spo11*-null pachytene spermatocytes is transcriptionally silenced.** (a and b) Cot1 RNA FISH staining detects nascent transcripts within the nucleus; the pseudo–sex body marked by γH2AX is a transcriptionally repressed domain. (c and d) In *Spo11*-null pachytene spermatocytes, as a result of asynapsis/nonhomologous synapsis, the two autosomal *Atr* loci are nearly always well separated. In the cell shown, there is a single *Atr* RNA FISH signal (arrows); DNA FISH shows that the second nontranscribing *Atr* locus lies within the pseudo–sex body domain (white outline). (e and f) A pachytene spermatocyte showing transcription of the Y chromosomal gene *Zfy2* when it is not located in the pseudo–sex body. (g and h) A nontranscribing *Zfy2* locus lying within the pseudo–sex body. (i–n) RNA/DNA FISH for the *Ddx3x/Usp9x* X chromosomal BAC showing two transcribing pachytene spermatocytes with the locus outside the pseudo–sex body and one nontranscribing pachytene spermatocyte in which the locus lies within the pseudo–sex body. (a–n) White outlines indicate the extent of the γH2AX domain before DNA FISH, and arrows point to the FISH signals (either RNA FISH or DNA FISH). Bar, 5 μm.

robust MSUC response covering the unsynapsed chromosome regions, including the unsynapsed X and Y axes (Fig. 3, a and b). However, with increasing asynapsis, the unsynapsed chromatin–located γH2AX staining became progressively more fragmented and weaker, and this was associated with increasingly focal ATR staining that was axially restricted without the spreading to adjacent chromatin that characterizes the MSUC response (Fig. 3, c–f). This fragmented γH2AX staining resembled that of meiotic DSB-associated γH2AX (Mahadevaiah et al., 2001). Amounts of γH2AX appeared to remain relatively constant in the face of increasing asynapsis; this was confirmed by quantitating the γH2AX signal (Fig. 3 i). Because the cells with fragmented and weak γH2AX staining had multiple regions of asynapsis and lacked a sex body or pseudo–sex body, we were concerned that they might have been zygotene spermatocytes, although there was often nonhomologous synapsis with the more extensive asynapsis (Fig. 3, e and f), which we consider a robust pachytene marker. For further confirmation, we stained testis tubule squashes for γH2AX and for the midpachytene marker histone H1t (Moens et al., 1997; Inselman et al., 2003), which appears during epithelial stage IV (Fig. S5, a–c; available at http://www.jcb.org/cgi/content/full/jcb.200710195/DC1). This confirmed that there were abundant H1t-positive *Dnmt3l*$^{-/-}$ spermatocytes that had fragmented γH2AX staining and no sex

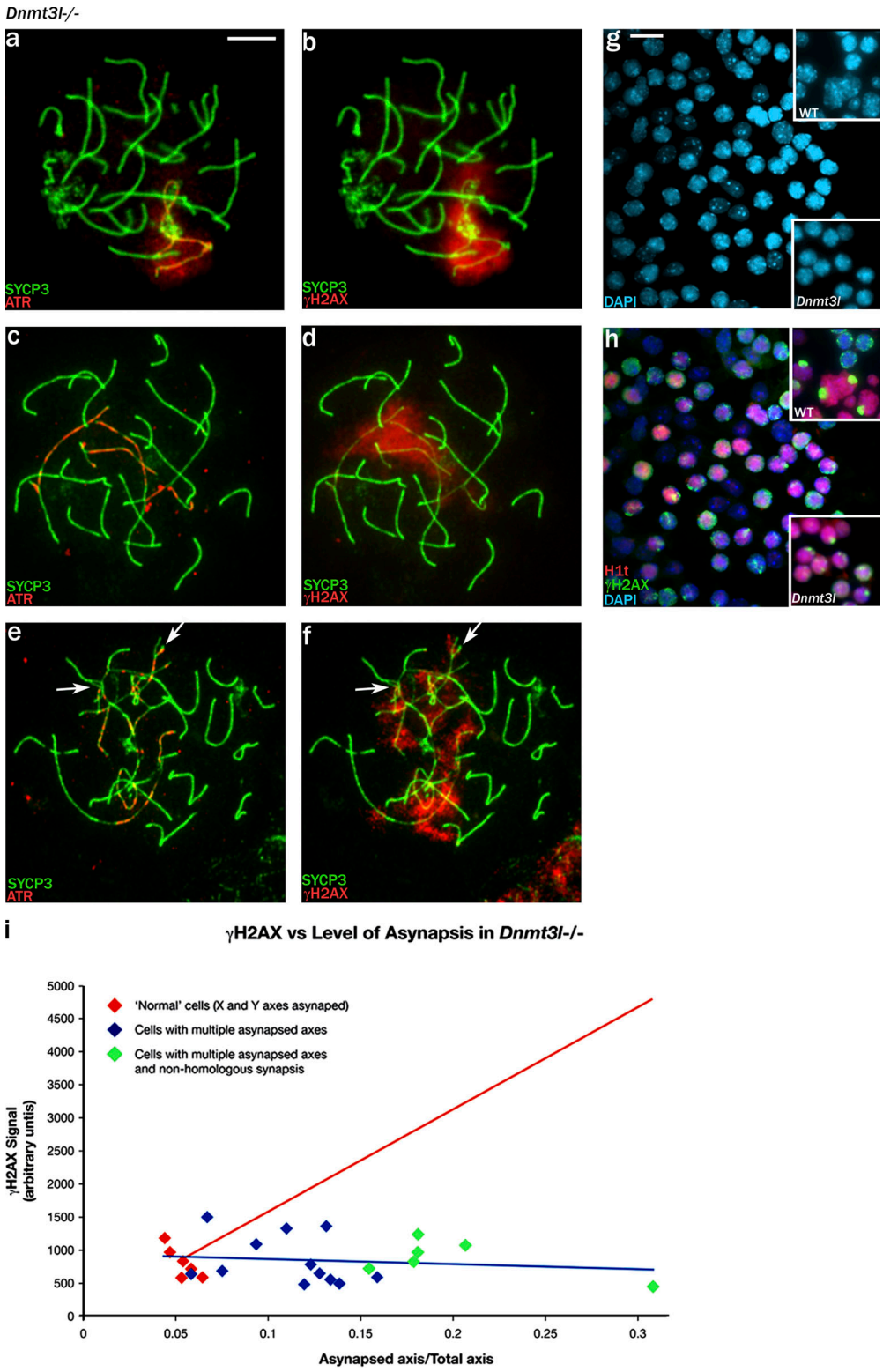

Figure 3. **In *Dnmt3l*-null pachytene spermatocytes, increasing levels of asynapsis attenuate the MSUC response.** (a and b) A rare pachytene spermatocyte with asynapsis restricted to what are probably the X and Y axes. ATR has been recruited to the asynapsed axes and has spread to the associated chromatin, and there is phosphorylation of H2AX throughout the associated chromatin. (c–f) With increasing asynapsis, the ATR becomes more focal and axially restricted, and the γH2AX staining becomes weaker and progressively more fragmented. Arrows indicate axes with partner exchange indicative of nonhomologous synapsis. (g and h) Staining of a spermatogenic cell squash preparation for the midpachytene marker H1t and for γH2AX shows that the majority of H1t-positive cells have fragmented γH2AX staining; only rare cells have a single sex body–like γH2AX-positive domain (bottom insets). In the control (top insets), cells with fragmented γH2AX staining (presumed to be zygotene) are H1t negative, whereas all H1t-positive spermatocytes have a single γH2AX-positive sex body (the small H1t-positive cells are round spermatids). (i) Quantitation of the whole nuclear γH2AX signal for rare pachytene spermatocytes with only the X and Y axes asynapsed and for pachytene spermatocytes with increasing levels of asynapsis shows that the amount of γH2AX does not increase in response to asynapsis (fitted blue regression line). The projected increase in γH2AX signal if it was in proportion to the amount of asynapsed axis is denoted by the red line. Bars: (a–f) 10 μm; (g and h) 15 μm.

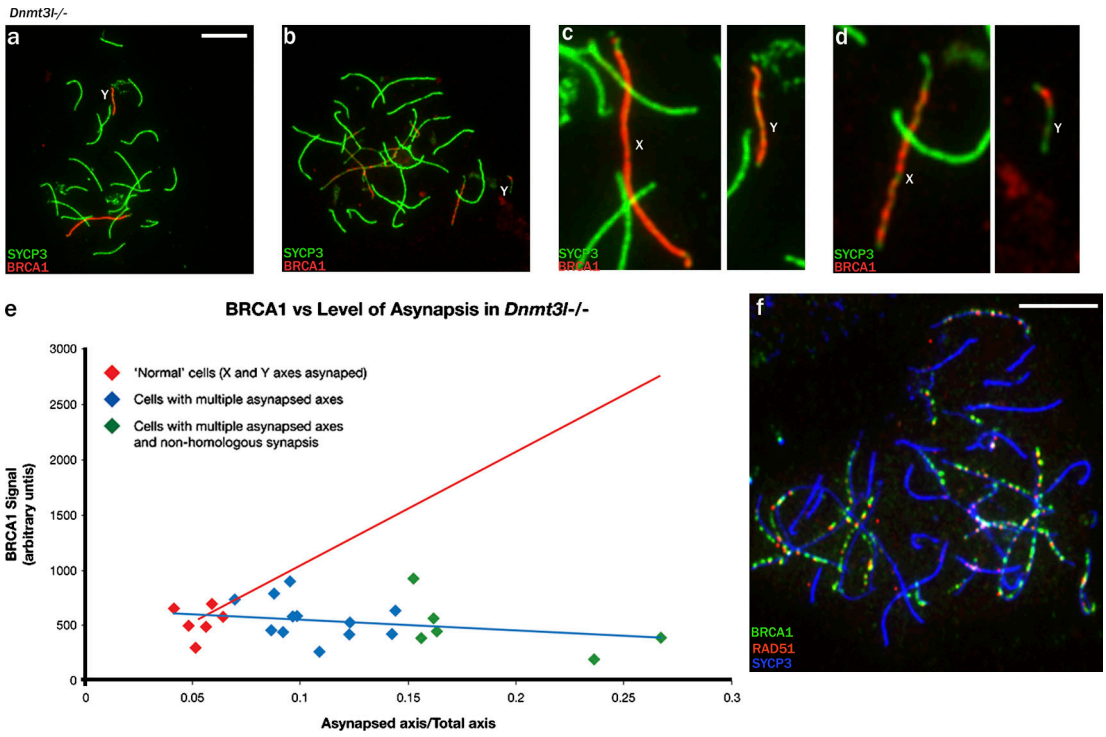

Figure 4. **Increasing asynapsis may attenuate the MSUC response by sequestering BRCA1 at unrepaired DSBs.** (a and b) In *Dnmt3l*$^{-/-}$ pachytene spermatocytes, increasing asynapsis is associated with increasingly focal BRCA1 staining. In the two spermatocytes shown, the Y chromosome has failed to synapse with the X chromosome. (c and d) Enlargements of the X (presumed) and Y chromosomes show that BRCA1 covers the axes of both chromosomes from the spermatocyte with only the X and Y asynapsed, but, in the spermatocyte with more extensive asynapsis, the BRCA1 has become more focal on the presumed X and is restricted on the Y chromosome to a single focus. (e) Quantitation of the axially located BRCA1 in pachytene spermatocytes shows that it does not increase with increasing asynapsis (fitted blue regression line). The projected increase in BRCA1 signal if it was in proportion to the amount of asynapsed axis is denoted by the red line. (f) The focal BRCA1 staining seen when asynapsis is extensive is largely DSB associated, as indicated by costaining for RAD51. Bars, 10 µm.

body; only rare midpachytene cells with a single sex body–like domain were seen (Fig. 3, g and h). Previously, Bourc'his and Bestor (2004) failed to detect H1t-positive *Dnmt3l*$^{-/-}$ spermatocytes with the same antibody, but they used spread cell preparations in which we have found that the weak stage IV H1t staining is not apparent.

Our finding that the amount of γH2AX does not increase in response to asynapsis (Fig. 3 i), even though in spermatocytes H2AX has been shown to be abundant throughout the nucleus (Fernandez-Capetillo et al., 2003), suggests that something is limiting the phosphorylation of H2AX by ATR. This could be limited availability of ATR itself or of BRCA1, which is involved in ATR recruitment to asynapsed axes (Turner et al., 2004). We have used RNA FISH to assess *Atr* and *Brca1* transcription (Fig. S2, a–j); *Atr* is robustly transcribed throughout pachytene, but *Brca1* transcription is shut down in the course of pachytene. More importantly, with increasing asynapsis in *Dnmt3l*$^{-/-}$ pachytene spermatocytes, it was apparent that the BRCA1 staining associated with these asynapsed axes became weaker and more focal (Fig. 4, a and b). Quantitation of the axially located BRCA1 in pachytene spermatocytes confirmed that it does not increase concomitantly with increasing asynapsis (Fig. 4 e). Because recruitment of ATR to the axes during the MSUC response is dependent on the prior recruitment of BRCA1, this strongly implicates BRCA1 recruitment to the asynapsed axes as the limiting factor.

In pachytene spermatocytes with extensive asynapsis, we suspected that the remaining focal BRCA1 was DSB associated. To see whether this was the case, we used combined staining for BRCA1 and the DSB-associated recombinase RAD51, once again using SYCP3 to stain the axes, and selected a pachytene cell with extensive asynapsis (Fig. 4 f). 108/137 (79%) BRCA1 foci were closely associated with RAD51 foci. In addition to the 29 BRCA1 foci not associated with RAD51, there were three RAD51 foci that were not associated with BRCA1.

The spermatocytes in Fig. 4 (a and b) were selected because they each had the Y chromosome as a univalent. In the higher magnification view of the sex chromosomes in these spermatocytes (Fig. 4, c and d), it is apparent that the Y from the spermatocyte with limited asynapsis is fully coated with BRCA1 (Fig. 4 c), but in the cell with more extensive asynapsis, the Y now has a single BRCA1 focus at one end (Fig. 4 d). We would argue that this Y chromosome has not been subjected to MSUC/MSCI because BRCA1 is now largely sequestered at the many unrepaired DSBs in this cell.

In the majority of *Dnmt3l*$^{-/-}$ pachytene cells, the X and/or Y chromatin was not incorporated within a clear MSUC domain, so we expected that there would be extensive MSCI failure. Once again, we assessed this by gene-specific RNA FISH for Y-located *Zfy2* and X-located *Ddx3x/Usp9x*, the judgement as to whether the cells were in pachytene being made based on the DAPI and γH2AX staining before visualization of the RNA

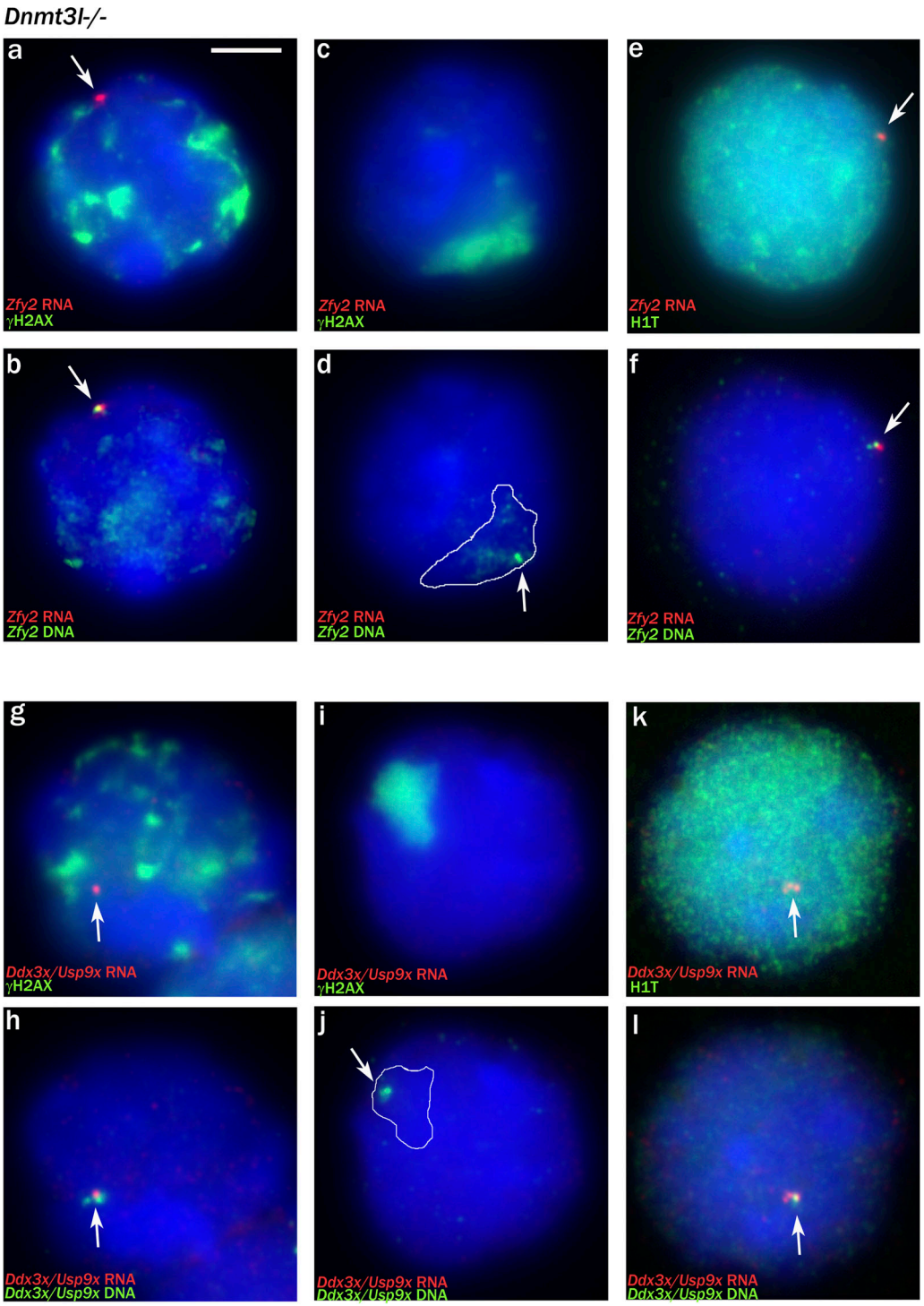

Figure 5. **The majority of *Dnmt3l*-null pachytene spermatocytes are transcribing X or Y genes (MSCI failure).** (a and b) RNA/DNA FISH showing strong *Zfy2* transcription in a spermatocyte with multiple γH2AX domains (note that some of the γH2AX staining has survived the DNA FISH procedure). (c and d) A rare pachytene spermatocyte with no *Zfy2* RNA FISH signal in which the *Zfy2* locus (arrow) lies within the sex body–like γH2AX domain (white outline). (e and f) An H1t-positive spermatocyte showing *Zfy2* transcription. (g and h) A pachytene spermatocyte with multiple γH2AX domains that is strongly expressing *Ddx3x/Usp9x*. (i and j) A pachytene spermatocyte with no *Ddx3x* RNA FISH signal with the locus within the sex body–like γH2AX-positive domain. (k and l) An H1t-positive spermatocyte showing *Ddx3x/Usp9x* transcription. (a–l) White outlines indicate the extent of the γH2AX domain before the DNA FISH, and arrows point to the FISH signals (either RNA FISH or DNA FISH). Bar, 5 μm.

FISH signal. As was the case in *Spo11*-null males, *Zfy2* was inappropriately expressed in the majority of these cells (53/55; 96%), including all six cells that we felt confident were pachytene cells based on the DAPI staining despite their having markedly fragmented γH2AX staining (Fig. 5, a and b). In the two cells that failed to express *Zfy2*, DNA FISH showed that the *Zfy2* locus lay within a sex body–like γH2AX-positive domain (Fig. 5, c and d). Similarly, the majority of cells (33/43; 77%)

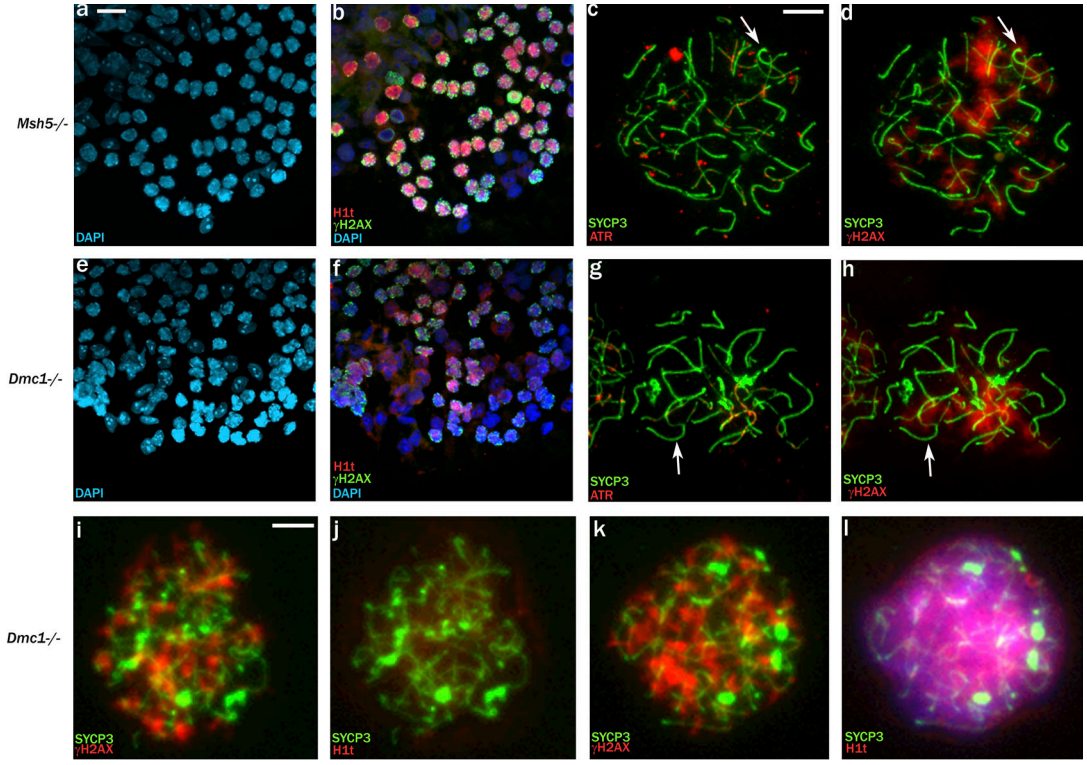

Figure 6. **Spermatocytes in *Msh5*- and *Dmc1*-null males reach midpachytene but do not mount an MSUC response.** (a and b) *Msh5*$^{-/-}$ spermatogenic cell squash preparation stained for H1t and γH2AX shows that the majority of H1t-positive cells have fragmented γH2AX staining. (c and d) A spread *Msh5*$^{-/-}$ spermatocyte judged to be in pachytene because there is some nonhomologous synapsis (arrows). ATR staining is focal and axially restricted, and the associated γH2AX staining is fragmented. (e and f) *Dmc1*$^{-/-}$ spermatogenic cell squash preparation stained for H1t and γH2AX shows many relatively weakly H1t-positive cells with fragmented γH2AX staining. (g and h) A spread *Dmc1*$^{-/-}$ spermatocyte judged to be in pachytene because there is some nonhomologous synapsis (arrows). ATR staining is again focal and axially restricted, and the associated γH2AX staining is fragmented. (i–l) *Dmc1*$^{-/-}$ surface-spread spermatocytes stained with a second H1t antibody reveals that cells with fragmented γH2AX staining can be either H1t negative (i and j) or positive (k and l). Bars: (a, b, e, and f) 15 µm; (c, d, and g–l) 10 µm.

were inappropriately expressing *Ddx3x/Usp9x*, including all four with fragmented γH2AX staining (Fig. 5, g and h). In the 10 nonexpressing cells, the *Ddx3x/Usp9x* locus lay within a sex body–like γH2AX domain (Fig. 5, i and j). As a further confirmation that many of the spermatocytes with fragmented γH2AX staining are pachytene cells and that these cells have MSCI failure, we repeated the *Ddx3x/Usp9x* analysis exclusively on cells with markedly fragmented γH2AX staining using relaxed selection criteria that included cells from late zygotene through to pachytene; 29/52 (56%) of these cells proved to be expressing *Ddx3x/Usp9x*.

Because *Zfy2* is expressed throughout zygotene in normal males, there is a danger that the estimate of MSCI failure is inflated by inclusion of late zygotene cells. Therefore, we attempted to perform RNA FISH in combination with H1t staining because H1t first appears during midpachytene and is less likely than other pachytene markers to be influenced by synaptic status. We were unable to get H1t staining to work in conjunction with RNA FISH using the antibody used on squashes, but we were successful with another antibody that was previously used successfully on spread spermatocytes (Inselman et al., 2003). Of the H1t-positive pachytene spermatocytes, 35/41 (85%) expressed *Zfy2* (Fig. 5, e and f). We also combined *Ddx3x/Usp9x* RNA FISH with H1t; 51/73 (70%) expressed *Ddx3x/Usp9x* (Fig. 5, k and l).

These results show that the presence of abundant DSBs on the asynapsed axes of *Dnmt3l*$^{-/-}$ pachytene spermatocytes has not facilitated the MSUC response to unsynapsed chromatin; indeed, there is a correlation between increasing levels of asynapsis and increasing impairment of the MSUC response. As a consequence, there is extensive MSCI failure (>70% of pachytene cells; least biased estimate of ∼85%).

Is MSCI failure the predominant cause of midpachytene spermatocyte apoptosis?

In *Spo11*$^{-/-}$ males, extensive apoptosis of spermatocytes occurs at epithelial stage IV, which equates with midpachytene in controls (Ashley et al., 2004a; Barchi et al., 2005). We have now shown that these males have MSCI failure, which has been clearly linked with midpachytene apoptosis (Turner et al., 2006), and this led us to consider whether MSCI failure is the predominant cause of epithelial stage IV apoptosis. H2AX-null males inevitably have MSCI failure because there is no H2AX protein to be phosphorylated in the XY chromatin domain; this is associated with pachytene apoptosis (Fernandez-Capetillo et al., 2003). We checked to see whether this also occurs at epithelial stage IV, and this proved to be the case (Fig. S5 e). We also found that the extensive MSCI failure we have identified in *Dnmt3l*$^{-/-}$ males is associated with stage IV spermatocyte apoptosis (Fig. S5 f).

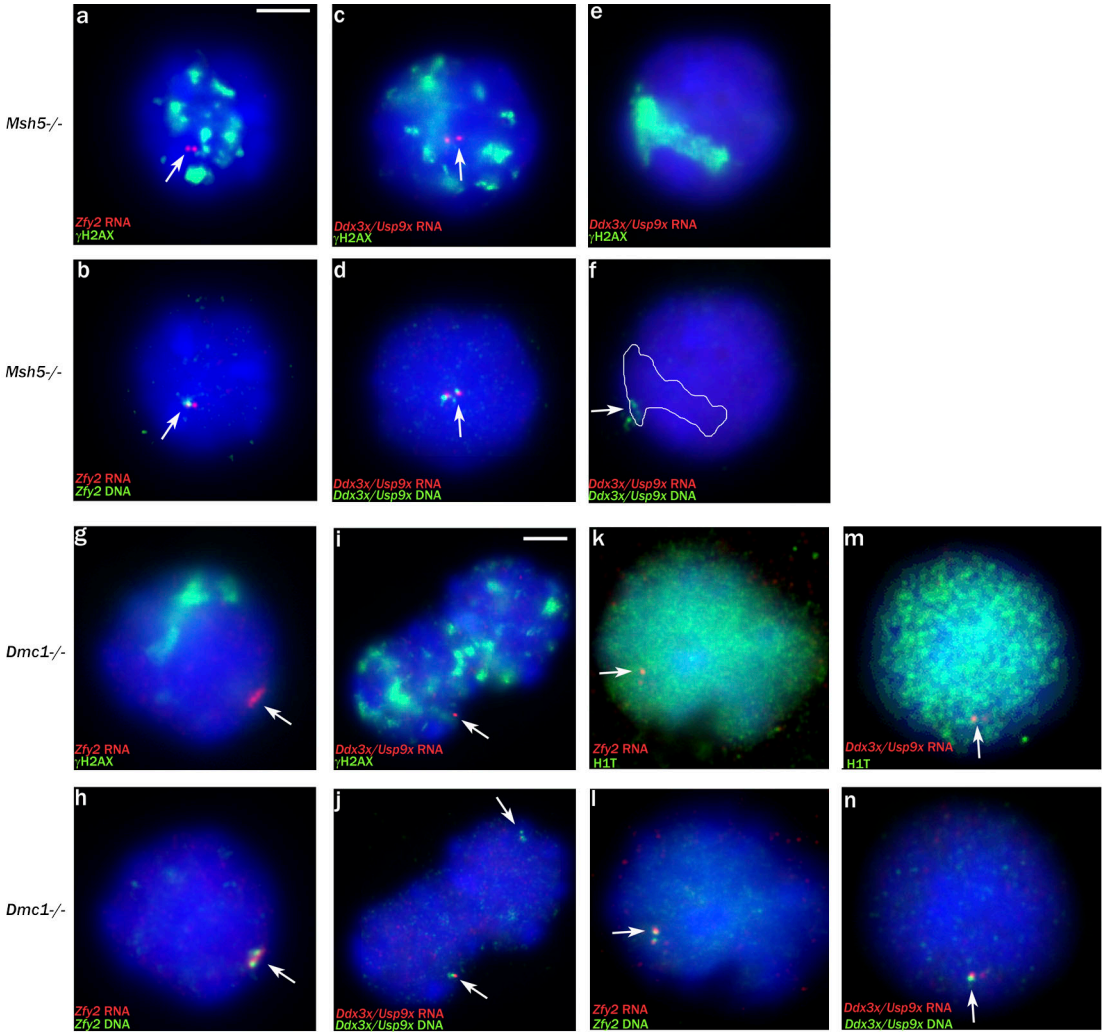

Figure 7. ***Msh5*- and *Dmc1*-null pachytene spermatocytes suffer from MSCI failure.** (a and b) *Zfy2* RNA/DNA FISH analysis showing transcription in an *Msh5*$^{-/-}$ spermatocyte with fragmented γH2AX staining, judged to be in pachytene; 59/60 (98%) transcribed *Zfy2*. (c and d) *Ddx3x/Usp9x* RNA/DNA FISH analysis showing transcription in an *Msh5*$^{-/-}$ pachytene spermatocyte with fragmented γH2AX staining; 44/49 (90%) transcribed *Ddx3x/Usp9x*. (e and f) *Ddx3x/Usp9x* RNA/DNA FISH analysis showing a nontranscribing *Msh5*$^{-/-}$ pachytene spermatocyte with the *Ddx3x/Usp9x* locus within a sex body–like γH2AX domain. (g and h) *Zfy2* RNA/DNA FISH analysis showing transcription in a *Dmc1*$^{-/-}$ spermatocyte judged to be in pachytene; 37/39 (95%) transcribed *Zfy2*. (i and j) *Ddx3x/Usp9x* RNA/DNA FISH analysis showing two *Dmc1*$^{-/-}$ pachytene spermatocytes with fragmented γH2AX staining, one transcribing and the second nontranscribing; 37/57 (65%) transcribed *Ddx3x/Usp9x*. (k and l) H1t-positive *Dmc1*$^{-/-}$ pachytene spermatocyte showing *Zfy2* transcription; 68/72 (92%) transcribed *Zfy2*. (m and n) H1t-positive *Dmc1*$^{-/-}$ pachytene spermatocyte showing *Ddx3x/Usp9x* transcription; 43/68 (63%) transcribed *Ddx3x/Usp9x*. (a–n) The white outline indicates the extent of the γH2AX domain before the DNA FISH, and arrows indicate FISH signals. Bars: (a–h and k–n) 5 µm; (i and j) 7 µm.).

In view of this link between MSCI failure and stage IV apoptosis, we decided to assess whether there is MSCI failure in *Msh5*$^{-/-}$ males and *Dmc1*$^{-/-}$ males, in which high levels of asynapsis are also associated with stage IV spermatocyte apoptosis (Pittman et al., 1998; Yoshida et al., 1998; Edelmann et al., 1999; de Vries et al., 1999; Barchi et al., 2005). It has previously been reported that the most advanced spermatocytes seen in *Msh5*$^{-/-}$ and *Dmc1*$^{-/-}$ males have fragmented γH2AX staining and lack sex bodies but that only those of *Msh5*$^{-/-}$ are H1t-positive (Barchi et al., 2005). Thus, it is not surprising that *Msh5*$^{-/-}$ testis tubule squash preparations immunostained for H1t and γH2AX showed abundant H1t-positive spermatocytes with fragmented γH2AX staining (Fig. 6, a and b). However, we also saw H1t-positive spermatocytes with fragmented γH2AX staining in *Dmc1*$^{-/-}$ testis tubule squashes, although the H1t staining was relatively weak (Fig. 6, e and f), and this was confirmed on spreads using the second H1t antibody (Fig. 6, i–l). This implies that spermatocytes in both mutants have reached a stage of pachytene consistent with epithelial stage IV (midpachytene), although the *Dmc1*$^{-/-}$ spermatocytes are arresting a little earlier in stage IV than those of *Msh5*$^{-/-}$. This is in agreement with our finding that in both mutants, some cells have achieved a degree of nonhomologous synapsis (Fig. 6, c and g). Once again, we have used *Zfy2* and *Ddx3x/Usp9x* RNA FISH to assay for MSCI failure (Fig. 7, a–n). Spermatocytes in both mutants express *Ddx3x/Usp9x*, which is a marker of pachytene cells with MSCI failure (Fig. 7, c, d, i, j, m, and n). In *Dmc1*$^{-/-}$, all of the putative pachytene cells have fragmented γH2AX staining, so we included an RNA FISH/H1t analysis for *Zfy2*; 68/72 (92%) H1t-positive spermatocytes transcribed *Zfy2*. These results provide compelling evidence that the most advanced cells in these

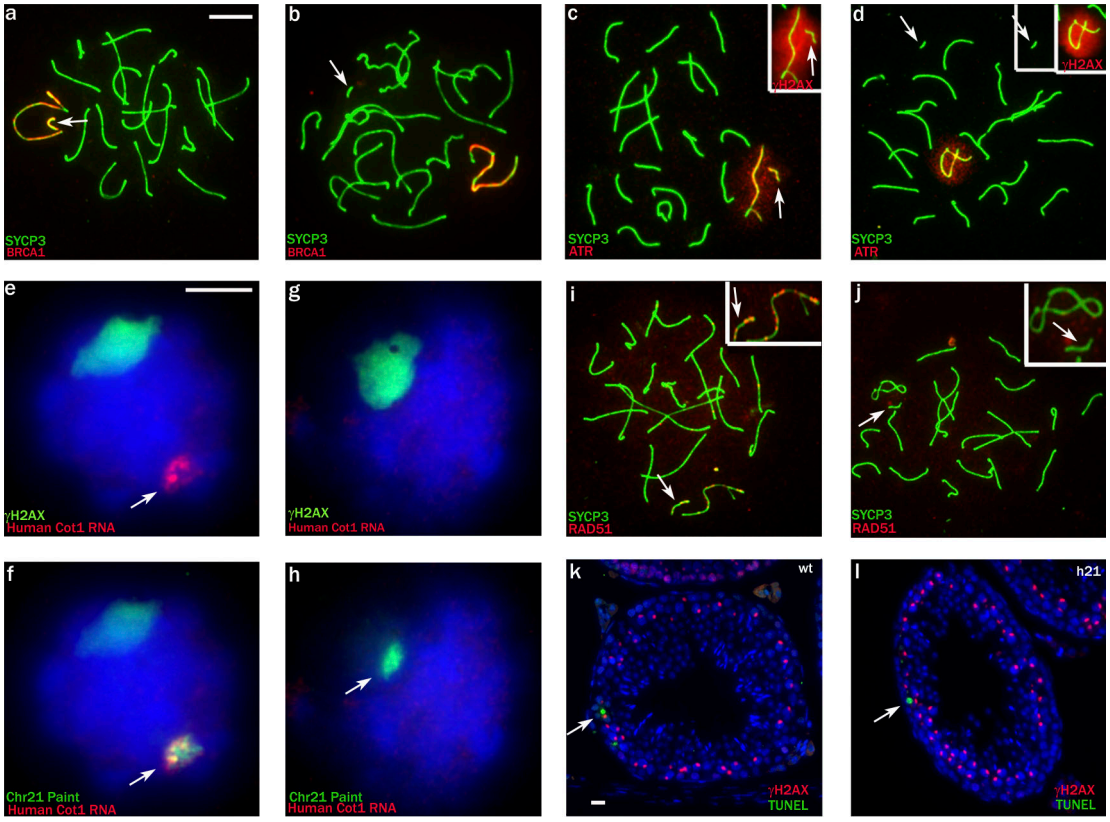

Figure 8. **The h21 chromosome of Down syndrome mice, when unsynapsed, has unrepaired DSBs and is transcriptionally silenced but does not invoke pachytene losses.** (a) Pachytene cell showing unsynapsed h21 (arrow), which is positive for BRCA1. (b) Pachytene cell with self-synapsed h21, which is negative for BRCA1. (c and d) The unsynapsed h21 is also positive for ATR and γH2AX (c; inset), whereas the self-synapsed h21 (d) is negative. (e and f) Human Cot1 RNA FISH/chromosome painting (arrows) showing that when h21 lies outside the γH2AX domain, it is transcriptionally active. (g and h) When h21 (arrow in h) lies within the γH2AX domain, it is transcriptionally silenced. (i) Pachytene cell showing RAD51 signals on the unsynapsed h21 and X chromosome; in the inset, the SCYP3 signal has been reduced so that the RAD51 foci are more visible. (j) In late pachytene, RAD51 signals disappear from both chromosomes. (i and j) In the insets, the SCYP3 signal is reduced to emphasize the lack of Rad51 staining. (k and l) In h21 carriers, apoptosis is not increased in stage IV tubules relative to controls (wt; arrows point to TUNEL-positive cells). (a–l) Arrows point to the h21. Bars: (a–d, i, and j) 10 μm; (e–h) 5 μm; (k and l) 40 μm.

mutants are pachytene spermatocytes with extensive asynapsis rather than zygotene spermatocytes and that these pachytene spermatocytes have MSCI failure.

Asynapsis of an additional chromosome provokes an effective MSUC response in pachytene spermatocytes without triggering an apoptotic response

The aforementioned results show that in a range of mouse models with extensive stage IV pachytene apoptosis, there is extensive MSCI failure, which is sufficient to explain the stage IV apoptosis. However, it does not rule out the possibility that unrepaired DSBs (aside from those normally present in the asynapsed X axis) also serve as a trigger for apoptosis at this stage. To test this, we used the Down syndrome mouse model (O'Doherty et al., 2005) that carries an additional chromosome comprising most of the human chromosome 21 (h21). Importantly, because this chromosome is additional to the mouse complement, silencing of the chromosome by MSUC will not lead to the loss of any essential gene functions and cause pachytene spermatocyte loss.

We first used SYCP3 staining combined with either BRCA1 or ATR together with γH2AX staining to assess whether the asynapsed h21 engendered an MSUC response. In 30/68 (44%) pachytene cells, the h21 axis was unsynapsed and positive for BRCA1 and in close proximity to the XY bivalent (Fig. 8 a). In 33/68 (49%) pachytene cells, the h21 was self-synapsed and BRCA1 negative and was located away from the XY bivalent. In the remaining 5/68 (7%) pachytene cells, the h21 was self-synapsed and negative for BRCA1 but was close to the XY domain. The combined γH2AX and ATR staining revealed that in 29/49 (58%) pachytene cells, the h21 was incorporated in a γH2AX/ATR domain (in 24 of which the h21 was unsynapsed); in all but one of these, the domain also included the X and Y asynapsed axes (Fig. 8 c). In the 20/49 (40%) cells in which γH2AX and ATR were not associated with h21, it was self-synapsed (Fig. 8 d).

We next used γH2AX staining combined with a human Cot1 RNA probe followed by an h21 paint to confirm that h21 chromosomes within γH2AX-positive domains were inactivated. 45/92 (49%) pachytene cells had a clear human Cot1 RNA signal located away from the single γH2AX-positive domain (Fig. 8, e and f); these cells are likely those in which the h21 was self-synapsed. 47/92 (51%) pachytene cells had no Cot1 signal; in 46 of these, the h21 was located within the single γH2AX domain (Fig. 8, g and h), and in one, it lay within a second small γH2AX domain.

To confirm that the asynapsed h21 chromosomes have unrepaired DSBs, we stained spread spermatocytes for SYCP3

and the DSB-associated protein RAD51. In early pachytene cells, a mean of 4.1 ± 1.3 RAD51 foci are seen on the asynapsed h21 axis; a further 9.3 ± 1.3 RAD51 foci are present on the asynapsed X chromosome axis (Fig. 8 i). Intriguingly, self-synapsis of h21 is associated with loss of the RAD51 foci (Fig. S4 e). Abundant cells with asynapsed h21 chromosomes survive through to late pachytene; the DSB-associated markers then disappear from h21 and from the asynapsed X chromosome axis (Fig. 8 j). We have used sections stained with DAPI and TUNEL to assess whether there is any excess pachytene apoptosis at epithelial stage IV in these h21 testes (Fig. 8, k and l), and there was no significant difference between the two genotypes (TUNEL-positive pachytene cells per tubule cross section: h21, 1.82 ± 0.91; wild type, 1.82 ± 0.74).

Discussion

Our initial objective was to see whether the presence of unrepaired meiotic DSBs on asynapsed axes is essential to trigger an MSUC response. Our analysis of *Spo11*$^{-/-}$ pachytene spermatocytes shows that a robust MSUC response can occur in the absence of *Spo11*-dependent meiotic DSBs. As befits an MSUC response, it was targeted to asynapsed axes, but it was restricted to only a small proportion of the asynapsed axes present. This *Spo11* independence is reminiscent of the *Spo11* independence of histone H3 methylation of lysine 9 that is a feature of the transcriptionally repressed X in pachytene spermatocytes of XO males in *Caenorhabditis elegans* (Reddy and Villeneuve, 2004) and of the *Spo11* independence of meiotic silencing by unpaired DNA in *Neurospora crassa* (Kelly and Aramayo, 2007).

Nevertheless, we did consider that the presence of unrepaired meiotic DSBs may potentiate the MSUC response. However, our analysis of *Dnmt3l*$^{-/-}$ pachytene spermatocytes showed that with increasing asynapsis and associated unrepaired DSBs, there is in fact a progressive impairment of the MSUC response. Triggering of the MSUC response has previously been shown to require the BRCA1-dependent recruitment of ATR to axes that remain asynapsed at the zygotene/pachytene transition (Turner et al., 2004). In the present study, we have found that the total amount of axially located BRCA1 remains constant in the face of increasing asynapsis. The resulting progressive diminution of the amount of BRCA1 per unit length of asynapsed axis with the consequent reduction in ATR recruitment provides an explanation for the progressive impairment of the MSUC response.

Why isn't the axial BRCA1 recruitment maintained in the face of increasing asynapsis? One possibility that we plan to investigate further is that the BRCA1 recruited to asynapsed axes at the zygotene/pachytene transition is normally derived from the pool of BRCA1 released from DSBs after synapsis rather than from a more general cellular pool. Under this model, the BRCA1 retained at unrepaired breaks in *Dnmt3l*$^{-/-}$ pachytene spermatocytes would then be unavailable for recruitment to asynapsed axes, thus accounting for abrogation of the MSUC response.

Because MSCI is a consequence of the MSUC response to the unsynapsed X and Y chromatin, this model for abrogation of the MSUC response by BRCA1 retention at unrepaired breaks provides an explanation for the observed MSCI failure in *Dnmt3l*-, *Msh5*-, and *Dmc1*-null males. There is now substantial evidence that MSCI failure is sufficient to cause stage IV (midpachytene) apoptosis in the absence of any significant increase in asynapsis or unrepaired DSBs. Thus, as we have shown here, the catastrophic pachytene failure in H2AX$^{-/-}$ males occurs at stage IV; these mice have MSCI failure because there is no H2AX to be phosphorylated, but they do not have obvious synaptic defects other than increased XY asynapsis (Fernandez-Capetillo et al., 2003). Further compelling evidence for the link between MSCI failure and midpachytene loss comes from the finding that in XYY males, there is selective loss of XYY pachytene cells with YY synapsis and associated inappropriate Y gene expression; XYY cells in which the two Ys remain unsynapsed (and thus are transcriptionally inactivated by MSUC) survive meiotic prophase (Turner et al., 2006). Our current finding of extensive MSCI failure in *Spo11*-null males also provides a sufficient explanation for the previously puzzling stage IV pachytene apoptosis in the absence of meiotic DSBs. It is important to emphasize that we are not asserting that MSCI failure is necessarily the only cause of stage IV pachytene apoptosis. Based on H1t staining, it is clear that in *Dmc1*$^{-/-}$ mutants, apoptotic elimination is completed earlier in stage IV than in *Msh5*$^{-/-}$ mutants. This could be because the more penetrant synaptic failure in *Dmc1*$^{-/-}$ leads to more complete MSCI failure. However, it could indicate the presence of an additional, as yet unidentified trigger for apoptosis that operates slightly earlier in stage IV.

In light of our findings, it is likely that MSCI failure is a predominant cause of midpachytene spermatocyte apoptosis. de Rooij and de Boer (2003) were the first to suggest that there is an epithelial stage IV checkpoint of pachytene spermatocytes that triggers the apoptotic elimination of aberrant cells. Since then, an increasing number of mutants have been shown to have substantial apoptosis at around this stage (de Vries et al., 1999; Ashley et al., 2004b; Hamer et al., 2004; Barchi et al., 2005; de Vries et al., 2005; Ahmed et al., 2007; Bolcun-Filas et al., 2007; Carmell et al., 2007). Kolas et al. (2004) have also pointed out that several such mutants have aberrant sex body morphology; this is almost certain to be associated with MSCI failure. In our view, for any mutants exhibiting elevated epithelial stage IV pachytene spermatocyte apoptosis, it will be necessary in the future to rule out MSCI failure before invoking other causes. Given the link between asynapsis and MSCI failure and that MSCI failure is necessarily a male-specific phenomenon, our results also go a long way toward explaining the more severe consequences of asynapsis for male as compared with female fertility in mice and men (Hunt and Hassold, 2002; Kolas et al., 2005; Morelli and Cohen, 2005).

What, then, is the response to unrepaired meiotic DSBs in pachytene spermatocytes in the absence of MSCI failure? The present analysis of mice carrying an additional h21-derived chromosome shows that these mice have a robust MSUC response that inactivates h21 (except when self-synapsed) together with the X and Y chromosomes. The approximately four unrepaired DSBs present on the asynapsed h21 chromosome do not trigger increased stage IV pachytene apoptosis. This is perhaps unsurprising because pachytene spermatocytes always have approximately nine unrepaired DSBs on the X that are tolerated.

At the level of the present analysis, the cellular response to the asynapsed h21 chromosome was in fact indistinguishable from the response to the unsynapsed region of the X chromosome. Thus, both were subject to MSUC, and RAD51 foci (indicative of unrepaired DSBs) were present in early and midpachytene, but these foci disappeared during late pachytene, suggesting that the DSBs were then repaired (presumably using the DNA strand of the sister chromatid as the repair template). Heterologous self-synapsis of h21, on the other hand, was associated with an earlier loss of RAD51 foci; this is also true after heterologous self-synapsis of the X chromosome (our unpublished data). We conclude that meiotic DSBs that remain unrepaired as a consequence of asynapsis when on chromosomes subject to MSUC do not trigger midpachytene spermatocyte apoptosis; repair of the DSBs in late pachytene will serve to avoid any subsequent DSB-related checkpoint response.

We should emphasize that we nevertheless subscribe to the view that there is a checkpoint operating in mammalian meiosis related to that in meiotic G2, which in spermatogenesis prevents progression to the first meiotic division (MI) while unrepaired breaks are present (for review see Burgoyne et al., 2007). We also presume that ATR is the key checkpoint kinase. As we have discussed elsewhere, we suspect that the ATR-rich sex body is a potent checkpoint signaling module that will prevent progression to MI and that loss of the sex body during diplotene (even though X and Y silencing is largely maintained via other chromatin modifications) is essential to allow progression to MI (for review see Burgoyne et al., 2007). Thus, during the tenure of the sex body, ATR signaling from any unrepaired DSBs may be irrelevant. In addition to a G2-related response to unrepaired DSBs, there may also be a checkpoint equivalent to that in budding yeast (Xu et al., 1997; Hochwagen and Amon, 2006) that detects stalled recombination intermediates. In this regard, there is an interesting recent report of a severely hypomorphic mutant of *Trip13* that leads to extensive pachytene failure in both sexes despite near-normal synapsis and an intact MSUC response (as indicated by the presence of sex bodies; Li and Schimenti, 2007). In this mutant, various markers of recombination intermediates were retained on the synapsed axes, showing that the process of homologous recombination was stalled (Li and Schimenti, 2007).

There are several unresolved questions with respect to the present and previous analyses of *Spo11*$^{-/-}$ male meiosis that warrant further investigation. First, there is our surprising finding of BRCA1 foci on the forming axial elements despite the absence of meiotic (*Spo11* dependent) DSBs; it would be fascinating to know what underlies this BRCA1 localization. Of more relevance to the present study is the question as to why there is a robust but spatially limited BRCA1 recruitment to asynapsed chromatin (to form the pseudo–sex body). BRCA1 is a very large protein with several functionally separable domains, including a C-terminal BRCT domain and a central DNA-binding domain, between which is an SQ/TQ cluster domain (SCD); the latter includes phosphorylation sites for ATM and ATR (for review see Burgoyne et al., 2007). The localization of BRCA1 to DSBs is likely to involve binding to γH2AX in the vicinity of the break via the BRCT domain and/or binding to specific DNA structures at the break via the DNA-binding domain. In the model we have suggested here, it is BRCA1 released from meiotic DSBs after synapsis that is normally recruited in a meiotic DSB-independent manner to unsynapsed axes to initiate the MSUC response. In *Brca1*$^{\Delta 11/\Delta 11}$,*Trp53*$^{+/-}$ males, which lack the region encoding the SCD, the shortened BRCA1 protein is nevertheless still recruited to the asynapsed axes of the X and Y (Turner et al., 2004; Fig. S2 b). Thus, the SCD is not needed for this axial BRCA1 recruitment but is required for the subsequent axial recruitment of ATR. In *Spo11*$^{-/-}$ males, BRCA1 still appears (as foci) on the unsynapsed axes as soon as they form in leptotene and is subsequently shed from regions of synapsis. However, because it has not been associated with meiotic DSBs, it is likely that the SCD may not be phosphorylated at those sites normally phosphorylated by ATM and/or ATR. We have observed that one or a few clumps of ATR are present in the nuclei of late zygotene *Spo11*$^{-/-}$ spermatocytes, and we hypothesize that this ATR is needed to phosphorylate one or more sites in the BRCA1 SCD that are critical for subsequent axial recruitment of ATR. Under this model, the formation of a pseudo–sex body thus depends on the colocalization of asynapsed axes that recruit BRCA1 with one of these ATR clumps.

Materials and methods

Mice

The *Spo11*- (Baudat et al., 2000) and *Dnmt3l* (Bourc'his et al., 2001)-null mutations were on a C57BL/6 background, the *Msh5*- (Edelmann et al., 1999) and *Dmc1* (Pittman et al., 1998)-null mutations were on a mixed C57BL/6 + 129/Sv background, the *Brca1*$^{\Delta 11}$ mutation (Xu et al., 2001) together with the accompanying *Trp53*-null mutation (Donehower et al., 1992) was on a mixed C57BL/6 + 129/Sv + Black Swiss background (National Institutes of Health), and the h21 chromosome (O'Doherty et al., 2005) on a predominantly random bred MF1 (National Institute for Medical Research colony) background. Mutant testes and litter mate controls were processed at the following ages: *Msh5* and *Dmc1*, young adults; *Spo11*, 16 d postpartum (in older males there was general transcriptional repression during pachytene, which reduced the RNA FISH signals); *Dnmt3l*, 25–30 d postpartum (before severe spermatogenic failure seen in older males); *Brca1*$^{\Delta 11}$, 21 d postpartum male; *h21* carrier, 34 d postpartum. Other normal testis material was from random bred MF1 (National Institute for Medical Research colony) males processed as young adults.

Immunofluorescent staining

Surface spreads were prepared as described in Barlow et al. (1997). All testis material from the mutants and litter mate controls had been frozen in liquid nitrogen before use. The *Msh5*, *Dmc1*, and *Brca1*$^{\Delta 11/\Delta 11}$,*Trp53*$^{+/-}$ mutant testes were archived frozen testes remaining from previous studies (Turner et al., 2004; Barchi et al., 2005). Samples of the frozen testes were thawed in RPMI medium before use. All primary antibody incubations were performed overnight at 37°C, and secondary antibody incubations were performed for 1 h at 37°C. Primary antibodies used were rabbit polyclonal anti-SYCP3 (1:100; Abcam), mouse monoclonal anti-SYCP3 (1:100; Abcam), rabbit polyclonal anti-SYCP1 (1:100; Abcam), mouse monoclonal anti-RAD51 (1:10; Abcam), rabbit polyclonal anti-RPA32 (1:100; Abcam), rabbit polyclonal anti-BRCA1–1,059 (1:100; Turner et al., 2004), rabbit polyclonal anti-H1t (1:200; Moens et al., 1997), guinea pig polyclonal anti-H1t (1:1,000; Inselman et al., 2003), goat polyclonal anti-ATR (1:100; Santa Cruz Biotechnology, Inc.), and mouse monoclonal anti-γH2AX (1:100; Millipore). Secondary antibodies used were from the AlexaFluor Dye series (Invitrogen), and all were used at 1:500. Slides were mounted in Vectashield with DAPI (Vector Laboratories).

Distinguishing spread pachytene spermatocytes with synaptic errors from zygotene spermatocytes

The pachytene stage is defined as beginning when autosomal synapsis is completed; this criterion cannot be used in mutants with asynapsis. Because MSCI is impaired with higher levels of asynapsis, the morphology of the XY bivalent/sex body also cannot be used to differentiate between late zygotene

and early pachytene. Instead, we used the following criteria to identify pachytene cells in spread preparations. (1) DAPI staining pattern: during leptotene/zygotene, DAPI staining is bright throughout the nucleus, and centromeres are clustered in a few subdomains. In contrast, pachytene nuclei have more heterogeneous DAPI staining, with euchromatin more faintly stained and centromeres brightly stained and separated into multiple subdomains (Turner et al., 2001). (2) The length and thickness of axial elements/synaptonemal complexes: axial elements appear long and thin in leptotene and zygotene, whereas those of pachytene cells are shorter and thicker (Ashley et al., 2004a). (3) Pachytene cells with asynapsis can also be discriminated from zygotene cells by the presence of markedly asynchronous synapsis between individual bivalents (for example, completely asynapsed bivalents in the presence of multiple fully synapsed bivalents). (4) We view the presence of nonhomologous synapsis (particularly evident in *Spo11*$^{-/-}$) and/or evidence of a robust MSUC response because both of these processes initiate close to the zygotene–pachytene transition (Zickler and Kleckner, 1999; Turner et al., 2005) as definitive criteria, but they often cannot be used for pachytene cells with extensive asynapsis.

γH2AX and BRCA1 quantitation

To select *Dnmt3l*$^{-/-}$ pachytene cells for quantitation, the SYCP3 signal and then the DAPI signal were viewed under a 40× objective. Any cells judged from the SYCP3/DAPI staining to be pachytene cells were marked. The marked cells were subsequently analyzed under a 100× objective, and images were captured for those judged to be sufficiently spread and undamaged (assessed from the DAPI image) for subsequent quantitative analysis. The amount of fluorescence was measured from the captured images using the integrated density feature of the Softworx software of the DeltaVision microscope (Applied Precision). For measuring nuclear anti-γH2AX fluorescence, each nucleus was outlined, and the total fluorescence was measured within this outline; for each nucleus background, fluorescence (estimated for an equivalent area in the near vicinity of the nucleus) was subtracted. To measure the amount of BRCA1, which is present on the asynapsed axial elements, the outlines of all of the asynapsed axes were carefully traced, and the anti-BRCA1 fluorescence within the areas covered by these outlines was measured. A sample of synapsed axes in each nucleus was also outlined from which the background subtraction was calculated. The lengths of the synapsed regions and of unsynapsed axial elements were measured using the ImageJ program (National Institutes of Health). The unsynapsed axial element length was expressed as a proportion of the total axial element length (unsynapsed axial element length + twice the length of the synapsed regions) for each nucleus.

RNA and DNA FISH with immunostaining

Cot1 RNA FISH or gene/BAC-specific RNA FISH was followed by γH2AX immunostaining or H1t staining (guinea pig anti-H1t; 1:500) and then by DNA FISH as previously described (Turner et al., 2005, 2006). BAC probes used for RNA/DNA FISH were as follows: *Ddx3x/Usp9x*, CITB-551M19; *Zfy2*, CITB-288D7 (Research Genetics); *Atr*, RP24-3994J4 (CHORI); and *Brca1*, BMq-359C01 (Gene Services). For γH2AX-stained cells, a judgement as to meiotic stage was made from the γH2AX staining pattern (in the case of mutants, taking into account the pattern expected based on the analysis of spread cells) together with the DAPI staining pattern before the DNA FISH procedure.

TUNEL analysis

TUNEL analysis was performed on 5-µm paraffin sections of dilute Bouins fixed testes according to the manufacturer's protocol (In Situ Cell Death Detection kit; Roche). Adjacent sections were used for a periodic acid Schiff staining to identify epithelial stage IV tubules for quantitation.

Image acquisition

Cells were examined and digitally imaged on an inverted microscope (IX70; Olympus) with a 100-W mercury arc lamp using a 100× 1.35 U-PLAN-APO oil immersion objective (Olympus). Each fluorochrome image (AlexaFluor488, -555, -594, and -647 dyes) was captured separately as a 12-bit source image using a computer-assisted (DeltaVision) liquid-cooled (−40°C) CCD camera (CH350L; Photometrics) with a sensor (1,317 × 1,035 pixels; KAF1400; Kodak). A single multiband dichroic mirror was used to eliminate shifts between different filters. Captured images were processed using Photoshop 5.0.2 (Adobe).

Online supplemental material

Fig. S1 shows immunostaining for the DSB-associated proteins replication protein A and RAD51 in premeiotic S phase and leptotene spermatocytes from controls, *Spo11*$^{-/-}$, and *Dnmt3l*$^{-/-}$. Fig. S2 shows the assessment of *Atr*, *Brca1*, *Zfy2*, and *Ddx3x/Usp9x* transcription in control spermatocytes by RNA FISH. Fig. S3 shows *Zfy2* and *Ddx3x/Usp9x* transcription in *Brca1*$^{\Delta 11/\Delta 11}$ pachytene spermatocytes. Fig. S4 shows *Ddx3x/Usp9x* transcription analysis combined with H1t staining in wild-type and *Brca1*$^{\Delta 11/\Delta 11}$ mutant testes and self-synapsis of h21 in Down syndrome mouse pachytene spermatocytes. Fig. S5 shows the onset of H1t expression at testis epithelial stage IV and the elimination of pachytene spermatocytes at this stage in *H2ax*- and *Dnmt3l*-null mice. Online supplemental material is available at http://www.jcb.org/cgi/content/full/jcb.200710195/DC1.

We thank O. Ojarikre and A. Rattigan for mouse breeding and genotyping; P. Moens, C-X. Deng, and M. Handel for providing antibody reagents; M. Jasin, S. Keeney, and C-X. Deng for allowing us to use archived cryopreserved material from previous collaborative studies; and V. Tybulewicz for providing h21 carrier mice.

Submitted: 29 October 2007
Accepted: 26 June 2008

References

Ahmed, E.A., A. van der Vaart, A. Barten, H.B. Kal, J. Chen, Z. Lou, K. Minter-Dykhouse, J. Bartkova, J. Bartek, P. de Boer, and D.G. de Rooij. 2007. Differences in DNA double strand breaks repair in male germ cell types: lessons learned from a differential expression of Mdc1 and 53BP1. *DNA Repair (Amst.).* 6:1243–1254.

Ashley, T., A.P. Gaeth, L.B. Creemers, A.M. Hack, and D.G. de Rooij. 2004a. Correlation of meiotic events in testis sections and microspreads of mouse spermatocytes relative to the mid-pachytene checkpoint. *Chromosoma.* 113:126–136.

Ashley, T., C. Westphal, A. Plug-de Maggio, and D.G. de Rooij. 2004b. The mammalian mid-pachytene checkpoint: meiotic arrest in spermatocytes with a mutation in Atm alone or in combination with a Trp53 (p53) or Cdkn1a (p21/cip1) mutation. *Cytogenet. Genome Res.* 107:256–262.

Baarends, W.M., E. Wassenaar, R. van der Laan, J. Hoogerbrugge, E. Sleddens-Linkels, J.H. Hoeijmakers, P. de Boer, and J.A. Grootegoed. 2005. Silencing of unpaired chromatin and histone H2A ubiquitination in mammalian meiosis. *Mol. Cell. Biol.* 25:1041–1053.

Barchi, M., S. Mahadevaiah, M. Di Giacomo, F. Baudat, D.G. de Rooij, P.S. Burgoyne, M. Jasin, and S. Keeney. 2005. Surveillance of different recombination defects in mouse spermatocytes yields distinct responses despite elimination at an identical developmental stage. *Mol. Cell. Biol.* 25:7203–7215.

Barlow, A.L., F.E. Benson, S.C. West, and M.A. Hultén. 1997. Distribution of the RAD51 recombinase in human and mouse spermatocytes. *EMBO J.* 16:5207–5215.

Baudat, F., K. Manova, J.P. Yuen, M. Jasin, and S. Keeney. 2000. Chromosome synapsis defects and sexually dimorphic meiotic progression in mice lacking Spo11. *Mol. Cell.* 6:989–998.

Bellani, M.A., P.J. Romanienko, D.A. Cairatti, and R.D. Camerini-Otero. 2005. SPO11 is required for sex-body formation, and Spo11 heterozygosity rescues the prophase arrest of Atm−/− spermatocytes. *J. Cell Sci.* 118:3233–3245.

Bolcun-Filas, E., Y. Costa, R. Speed, M. Taggart, R. Benavente, D.G. de Rooij, and H.J. Cooke. 2007. SYCE2 is required for synaptonemal complex assembly, double strand break repair, and homologous recombination. *J. Cell Biol.* 176:741–747.

Bourc'his, D., and T.H. Bestor. 2004. Meiotic catastrophe and retrotransposon reactivation in male germ cells lacking Dnmt3L. *Nature.* 431:96–99.

Bourc'his, D., G.L. Xu, C.S. Lin, B. Bollman, and T.H. Bestor. 2001. Dnmt3L and the establishment of maternal genomic imprints. *Science.* 294:2536–2539.

Burgoyne, P.S., S.K. Mahadevaiah, and J.M. Turner. 2007. The management of DNA double-strand breaks in mitotic G(2), and in mammalian meiosis viewed from a mitotic G(2) perspective. *Bioessays.* 29:974–986.

Carmell, M.A., A. Girard, H.J. van de Kant, D. Bourc'his, T.H. Bestor, D.G. de Rooij, and G.J. Hannon. 2007. MIWI2 is essential for spermatogenesis and repression of transposons in the mouse male germline. *Dev. Cell.* 12:503–514.

de Rooij, D.G., and P. de Boer. 2003. Specific arrests of spermatogenesis in genetically modified and mutant mice. *Cytogenet. Genome Res.* 103:267–276.

de Vries, F.A., E. de Boer, M. van den Bosch, W.M. Baarends, M. Ooms, L. Yuan, J.G. Liu, A.A. van Zeeland, C. Heyting, and A. Pastink. 2005. Mouse Sycp1 functions in synaptonemal complex assembly, meiotic recombination, and XY body formation. *Genes Dev.* 19:1376–1389.

de Vries, S.S., E.B. Baart, M. Dekker, A. Siezen, D.G. de Rooij, P. de Boer, and H. te Riele. 1999. Mouse MutS-like protein MSH5 is required for proper chromosome synapsis in male and female meiosis. *Genes Dev.* 13:523–531.

Donehower, L.A., M. Harvey, B.L. Slagle, M.J. McArthur, C.A. Montgomery Jr., J.S. Butel, and A. Bradley. 1992. Mice deficient in p53 are developmentally normal but susceptible to spontaneous tumours. *Nature.* 356:215–221.

Edelmann, W., P.E. Cohen, B. Kneitz, N. Winand, M. Lia, J. Heyer, R. Kolodner, J.W. Pollard, and R. Kucherlapati. 1999. Mammalian MutS homologue 5 is required for chromosome pairing in meiosis. *Nat. Genet.* 21:123–127.

Fernandez-Capetillo, O., S.K. Mahadevaiah, A. Celeste, P.J. Romanienko, R.D. Camerini-Otero, W.M. Bonner, K. Manova, P. Burgoyne, and A. Nussenzweig. 2003. H2AX is required for chromatin remodeling and inactivation of sex chromosomes in male mouse meiosis. *Dev. Cell.* 4:497–508.

Hamer, G., H.B. Kal, C.H. Westphal, T. Ashley, and D.G. de Rooij. 2004. Ataxia telangiectasia mutated expression and activation in the testis. *Biol. Reprod.* 70:1206–1212.

Handel, M.A. 2004. The XY body: a specialized meiotic chromatin domain. *Exp. Cell Res.* 296:57–63.

Hata, K., M. Okano, H. Lei, and E. Li. 2002. Dnmt3L cooperates with the Dnmt3 family of de novo DNA methyltransferases to establish maternal imprints in mice. *Development.* 129:1983–1993.

Hata, K., M. Kusumi, T. Yokomine, E. Li, and H. Sasaki. 2006. Meiotic and epigenetic aberrations in Dnmt3L-deficient male germ cells. *Mol. Reprod. Dev.* 73:116–122.

Hochwagen, A., and A. Amon. 2006. Checking your breaks: surveillance mechanisms of meiotic recombination. *Curr. Biol.* 16:R217–R228.

Hunt, P.A., and T.J. Hassold. 2002. Sex matters in meiosis. *Science.* 296:2181–2183.

Inselman, A., S. Eaker, and M.A. Handel. 2003. Temporal expression of cell cycle-related proteins during spermatogenesis: establishing a timeline for onset of the meiotic divisions. *Cytogenet. Genome Res.* 103:277–284.

Keegan, K.S., D.A. Holtzman, A.W. Plug, E.R. Christenson, E.E. Brainerd, G. Flaggs, N.J. Bentley, E.M. Taylor, M.S. Meyn, S.B. Moss, et al. 1996. The Atr and Atm protein kinases associate with different sites along meiotically pairing chromosomes. *Genes Dev.* 10:2423–2437.

Kelly, W.G., and R. Aramayo. 2007. Meiotic silencing and the epigenetics of sex. *Chromosome Res.* 15:633–651.

Kolas, N.K., L. Yuan, C. Hoog, H.H. Heng, E. Marcon, and P.B. Moens. 2004. Male mouse meiotic chromosome cores deficient in structural proteins SYCP3 and SYCP2 align by homology but fail to synapse and have possible impaired specificity of chromatin loop attachment. *Cytogenet. Genome Res.* 105:182–188.

Kolas, N.K., E. Marcon, M.A. Crackower, C. Hoog, J.M. Penninger, B. Spyropoulos, and P.B. Moens. 2005. Mutant meiotic chromosome core components in mice can cause apparent sexual dimorphic endpoints at prophase or X-Y defective male-specific sterility. *Chromosoma.* 114:92–102.

La Salle, S., C.C. Oakes, O.R. Neaga, D. Bourc'his, T.H. Bestor, and J.M. Trasler. 2007. Loss of spermatogonia and wide-spread DNA methylation defects in newborn male mice deficient in DNMT3L. *BMC Dev. Biol.* 7:104.

Li, X.C., and J.C. Schimenti. 2007. Mouse pachytene checkpoint 2 (trip 13) is required for completing meiotic recombination but not synapsis. *PLoS Genet.* 3:e168.

Lisby, M., and R. Rothstein. 2005. Localization of checkpoint and repair proteins in eukaryotes. *Biochimie.* 87:579–589.

Mahadevaiah, S.K., J.M.A. Turner, F. Baudat, E.P. Rogakou, P. de Boer, J. Blanco-Rodriguez, M. Jasin, S. Keeney, W.M. Bonner, and P.S. Burgoyne. 2001. Recombinational DNA double-strand breaks in mice precede synapsis. *Nat. Genet.* 27:271–276.

Moens, P.B., D.J. Chen, Z. Shen, N. Kolas, M. Tarsounas, H.H.Q. Heng, and B. Spyropolous. 1997. Rad51 immunocytology in rat and mouse spermatocytes and oocytes. *Chromosoma.* 106:207–215.

Moens, P.B., M. Tarsounas, T. Morita, T. Habu, S.T. Rottinghaus, R. Freire, S.P. Jackson, C. Barlow, and A. Wynshaw-Boris. 1999. The association of ATR protein with mouse meiotic chromosome cores. *Chromosoma.* 108:95–102.

Morelli, M.A., and P.E. Cohen. 2005. Not all germ cells are created equal: aspects of sexual dimorphism in mammalian meiosis. *Reproduction.* 130:761–781.

O'Doherty, A., S. Ruf, C. Mulligan, V. Hildreth, M.L. Errington, S. Cooke, A. Sesay, S. Modino, L. Vanes, D. Hernandez, et al. 2005. An aneuploid mouse strain carrying human chromosome 21 with Down syndrome phenotypes. *Science.* 309:2033–2037.

Perera, D., L. Perez-Hidalgo, P.B. Moens, K. Reini, N. Lakin, J.E. Syvaoja, P.A. San-Segundo, and R. Freire. 2004. TopBP1 and ATR colocalization at meiotic chromosomes: role of TopBP1/Cut5 in the meiotic recombination checkpoint. *Mol. Biol. Cell.* 15:1568–1579.

Pittman, D.L., J. Cobb, K.J. Schimenti, L.A. Wilson, D.M. Cooper, E. Brignull, M.A. Handel, and J.C. Schimenti. 1998. Meiotic prophase arrest with failure of chromosome synapsis in mice deficient for Dmc1, a germline-specific RecA homolog. *Mol. Cell.* 1:697–705.

Plug, A.W., A.H. Peters, K.S. Keegan, M.F. Hoekstra, P. de Boer, and T. Ashley. 1998. Changes in protein composition of meiotic nodules during mammalian meiosis. *J. Cell Sci.* 111:413–423.

Reddy, K.C., and A.M. Villeneuve. 2004. *C. elegans* HIM-17 links chromatin modification and competence for initiation of meiotic recombination. *Cell.* 118:439–452.

Romanienko, P.J., and R.D. Camerini-Otero. 2000. The mouse Spo11 gene is required for meiotic chromosome synapsis. *Mol. Cell.* 6:975–987.

Scully, R., J. Chen, A. Plug, Y. Xiao, D. Weaver, J. Feunteun, T. Ashley, and D.M. Livingston. 1997. Association of BRCA1 with Rad51 in mitotic and meiotic cells. *Cell.* 88:265–275.

Turner, J.M., P.S. Burgoyne, and P.B. Singh. 2001. M31 and macroH2A1.2 co-localise at the pseudoautosomal region during mouse meiosis. *J. Cell Sci.* 114:3367–3375.

Turner, J.M., O. Aprelikova, X. Xu, R. Wang, S. Kim, G.V. Chandramouli, J.C. Barrett, P.S. Burgoyne, and C.X. Deng. 2004. BRCA1, histone H2AX phosphorylation, and male meiotic sex chromosome inactivation. *Curr. Biol.* 14:2135–2142.

Turner, J.M., S.K. Mahadevaiah, O. Fernandez-Capetillo, A. Nussenzweig, X. Xu, C.X. Deng, and P.S. Burgoyne. 2005. Silencing of unsynapsed meiotic chromosomes in the mouse. *Nat. Genet.* 37:41–47.

Turner, J.M., S.K. Mahadevaiah, P.J. Ellis, M.J. Mitchell, and P.S. Burgoyne. 2006. Pachytene asynapsis drives meiotic sex chromosome inactivation and leads to substantial postmeiotic repression in spermatids. *Dev. Cell.* 10:521–529.

Turner, J.M.A., and P.S. Burgoyne. 2007. Male meiotic sex chromosome inactivation and meiotic silencing. *In* The Y Chromosome and Male Germ Cell Biology in Health and Diseases. Y.-F.C. Lau and W.Y. Chan, editors. World Scientific Publishers, Hackensack, NJ. 27–45.

Webster, K.E., M.K. O'Bryan, S. Fletcher, P.E. Crewther, U. Aapola, J. Craig, D.K. Harrison, H. Aung, N. Phutikanit, R. Lyle, et al. 2005. Meiotic and epigenetic defects in Dnmt3L-knockout mouse spermatogenesis. *Proc. Natl. Acad. Sci. USA.* 102:4068–4073.

Xu, L., B.M. Weiner, and N. Klechner. 1997. Meiotic cells monitor the status of the interhomolog recombination complex. *Genes Dev.* 11:106–118.

Xu, X., W. Qiao, S.P. Linke, L. Cao, W.M. Li, P.A. Furth, C.C. Harris, and C.X. Deng. 2001. Genetic interactions between tumor suppressors Brca1 and p53 in apoptosis, cell cycle and tumorigenesis. *Nat. Genet.* 28:266–271.

Xu, X., O. Aprelikova, P. Moens, C.X. Deng, and P.A. Furth. 2003. Impaired meiotic DNA-damage repair and lack of crossing-over during spermatogenesis in BRCA1 full-length isoform deficient mice. *Development.* 130:2001–2012.

Yoshida, K., G. Kondoh, Y. Matsuda, T. Habu, Y. Nishimune, and T. Morita. 1998. The mouse RecA-like gene Dmc1 is required for homologous chromosome synapsis during meiosis. *Mol. Cell.* 1:707–718.

Zickler, D., and N. Kleckner. 1999. Meiotic chromosomes: integrating structure and function. *Annu. Rev. Genet.* 33:603–754.